Membrane wetting by biomolecular condensates is facilitated by mobile tethers

Trevor GrandPre,[1,2,*] Qiwei Yu,[1,*] Andrew G.T. Pyo,[2] Andrej Košmrlj,[3,4,†] and Ned S. Wingreen[1,5,‡]

[1] *Lewis-Sigler Institute for Integrative Genomics, Princeton University, Princeton, NJ 08544*
[2] *Department of Physics, Princeton University, Princeton, NJ 08544*
[3] *Department of Mechanical and Aerospace Engineering, Princeton University, Princeton, NJ 08544*
[4] *Princeton Materials Institute, Princeton University, Princeton, NJ 08544*
[5] *Department of Molecular Biology, Princeton University, Princeton, NJ 08544*

Biomolecular condensates frequently rely on membrane interactions for localization, recruitment, and chemical substrates. These interactions are often mediated by membrane-anchored mobile tethers, a feature overlooked by traditional wetting models. Here, we propose a general theoretical framework to study how mobile tethers impact both equilibrium and dynamic properties of condensate wetting. We show that a favorable tether-condensate interaction leads to tether enrichment at the condensate-membrane interface, which reduces the surface tension with the membrane and modifies the equilibrium contact angle. Increasing tether abundance on the membrane can drive transitions between wetting regimes, with only a modest binding energy required for biologically relevant scenarios. Furthermore, by helping condensates coat membranes, mobile tethers can facilitate condensate localization to junctions of membrane structures, such as the reticulated membranes inside the algal pyrenoid. These results provide a framework to study the implications of tether-mediated condensate-membrane interactions for cellular organization and function.

Biomolecular condensates, intracellular compartments formed via phase separation, are essential for diverse biological processes, including gene regulation, metabolism, and cell signaling [1, 2]. In many instances, proper condensate function relies on interactions with membranes [3, 4]. These membrane interactions can spatially organize condensates, concentrate interaction partners, and facilitate access to reactants. The algal pyrenoid exemplifies this interplay: condensates enriched with the CO_2-fixing enzyme Rubisco form around traversing membranes that supply CO_2 to enhance photosynthetic efficiency. Conversely, condensates can also facilitate membrane processes such as transport, signaling, force generation, and structural remodeling. For example, Focal Adhesion Kinase (FAK) forms condensates on the cytoplasmic membrane, binding to lipids at sites where focal adhesions assemble, thereby regulating cell motility [5]. Similarly, B cell activation involves condensation on the plasma membrane that is essential for downstream signaling [2]. More broadly, unraveling the dynamic relationship between condensates and membranes is proving to be essential for understanding intracellular organization and function.

In many cases, membrane-associated condensates do not directly wet membranes. Instead, they adhere to membrane surfaces via tethering molecules, such as proteins or specific lipids, that are anchored to the membrane. In the pyrenoid of the model alga *Chlamydomonas reinhardtii*, for example, pyrenoid-traversing membranes feature tethers like RBMP1, RBMP2, and SAGA1, which directly bind to Rubisco [6, 7]. These tether proteins are important for the structure and function of the pyrenoid condensate. Since membranes are typically fluid, tethers such as these are likely to be mobile within the membrane. Here, we seek to address the general question of how mobile tethers affect the condensate-membrane interaction and wetting.

In classical wetting theory, the contact angle θ is determined by the force balance at the three-phase junction through the Young-Dupré equation [8], which relates θ to the difference of surface tensions (Fig. 1A). In the presence of mobile tethers, however, favorable tether-condensate interactions enrich tethers within a condensate that wets the membrane (Fig. 1A), thereby creating a surface with inhomogeneous wetting properties. Specifically, tethers reduce the surface tension with both the dense and dilute phases, but differentially affect the dense phase more. Thus, tethers affect both the equilibrium contact angle and the nonequilibrium relaxation dynamics as a droplet wets a membrane. However, it has not been clear to what extent tethers can control wetting properties.

To address this question, we construct a general theoretical framework that describes the densities of tethers and condensates with phase fields ψ and ϕ, respectively. A high (lower) value of ϕ corresponds to a condensate dense (dilute) phase. The interactions are captured by a total free energy

$$\begin{aligned}\beta F =& c_{\psi,0}\int \mathrm{d}A\left[f_\psi(\psi)+\frac{\lambda_\psi}{2}(\nabla\psi)^2 - E(\psi,\phi|_{\mathrm{surf}})\right] \\ &+ c_{\phi,0}\int \mathrm{d}V\left[f_\phi(\phi)+\frac{\lambda_\phi}{2}(\nabla\phi)^2\right],\end{aligned} \tag{1}$$

where the first integral is over the membrane area, and the second integral is over the bulk volume. Energy is measured in units of $\beta^{-1} = k_{\mathrm{B}}T$. $c_{\psi,0}$ and

* These authors contributed equally to this work.
† andrej@princeton.edu
‡ wingreen@princeton.edu

$c_{\phi,0}$ are reference concentrations for the tether and condensate so that the free energy densities are non-dimensionalized: $E(\psi, \phi|_{\text{surf}})$ captures both condensate-tether and condensate-surface interactions; $f_\psi(\psi)$ and $f_\phi(\phi)$ are the free energy densities of tethers and condensates respectively; λ_ψ and λ_ϕ are constants associated with interface energies.

The model encompasses a large class of systems and interactions by allowing the free energy densities $f_\psi(\psi)$, $f_\phi(\phi)$, and the interaction energy $E(\psi, \phi|_{\text{surf}})$ to take any form. By minimizing the free energy in Eq. 1, we obtain the equilibrium concentration profile, from which the contact angle θ can be measured (Fig. 1B). To study the dynamics of wetting, we can further prescribe conserved (model B) dynamics [9]:

$$\partial_t \psi = \nabla \cdot (M_\psi \nabla \mu_\psi), \quad \partial_t \phi = \nabla \cdot (M_\phi \nabla \mu_\phi), \tag{2}$$

where M_ψ and M_ϕ are mobility coefficients, and $\mu_\psi = \delta F/\delta\psi$ and $\mu_\phi = \delta F/\delta\phi$ are the chemical potentials of the tethers and condensate, respectively.

To illustrate the physical picture, we study a minimal scenario of tether-mediated wetting. We consider a linear interaction energy $E(\psi, \phi) = (h_0 + h_1\psi)\phi$, where h_0 and h_1 describe condensate-membrane and condensate-tether interactions, respectively. We use Flory-Huggins free energies for self-energies $f_\xi(\xi) = \xi \ln \xi + (1-\xi)\ln(1-\xi) + \chi_\xi \xi(1-\xi)$, with $\xi \in \{\psi, \phi\}$ representing the area or volume fraction of tether and condensate, respectively [10]. We set the units of free energy densities via $c_{\psi,0} k_{\text{B}} T = 1$ and $c_{\phi,0} k_{\text{B}} T = 1$. Further assuming non-self-interacting mobile tethers ($\chi_\psi = 0$, $\lambda_\psi = 0$), we arrive at a minimal model for interrogating how tethers affect condensate wetting. However, we emphasize that the reported qualitative behaviors are generic and not sensitive to the specific choice of the functions for free energy densities and condensate-tether interaction energy.

Phase separation creates dense and dilute phases in the bulk, with binodal concentrations ϕ_{l} and ϕ_{g} (as measured in volume fractions), respectively. The concentration difference $\Delta\phi = \phi_{\text{l}} - \phi_{\text{g}}$ drives the attraction of tethers to the condensate, resulting in a volume fraction ψ_{l} in the dense phase, which is higher than that in the dilute phase ψ_{g} (Fig. 1A). This partition of tethers reaches equilibrium when chemical potentials are balanced: $\mu_{\psi,\text{l}} = \mu_{\psi,\text{g}}$, where $\mu_{\psi,*} = \delta F/\delta\psi_*$ for $* \in \{\text{l}, \text{g}\}$, which leads to (see *SI Appendix* for details)

$$\psi_{\text{l}} = \frac{\psi_{\text{g}} e^{h_1 \Delta\phi}}{1 + \psi_{\text{g}}(e^{h_1\Delta\phi} - 1)}, \tag{3}$$

where we have approximated the condensate concentrations at the surface with the binodal concentrations. This agrees well with numerical simulations across a wide range of ψ_{g}, for both repelling ($h_0 < 0$) or attracting ($h_0 > 0$) interactions between the bare membrane and the condensate (Fig. 1C).

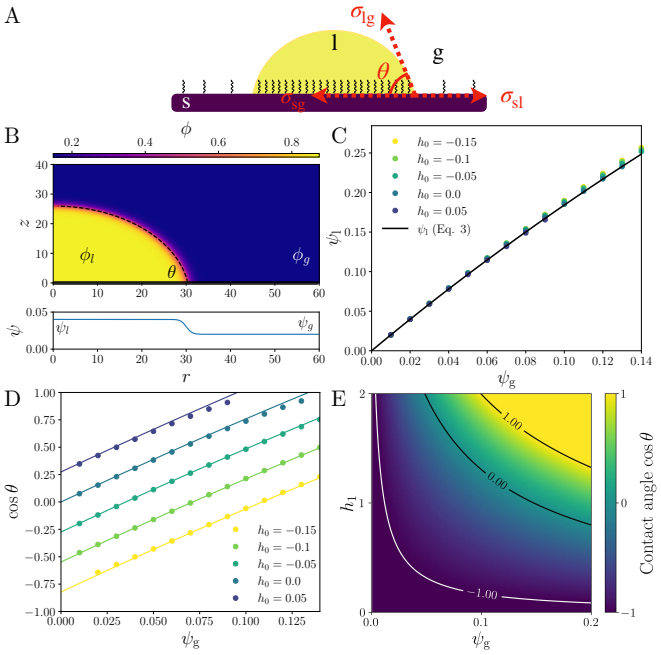

FIG. 1. Tether-mediated condensate wetting of membranes. (A) Illustration of a biomolecular condensate (yellow) interacting with tether molecules (black) to wet a membrane (purple). The interaction creates a localized enrichment of tethers around the condensate, surrounded by a lower background concentration of tethers. s, l, and g represent membrane ("solid"), dense phase ("liquid"), and dilute phase ("gas"). The contact angle θ is given by force balance at the three-phase junction: $\sigma_{\text{lg}} \cos\theta = \sigma_{\text{sg}} - \sigma_{\text{sl}}$, where σ represents surface tensions. (B) A typical equilibrium concentration profile obtained from numerical simulations. The condensate field ϕ (top) and tether field ψ (bottom) are plotted in cylindrical coordinates (r, z) with axial symmetry. The thick black line indicates the membrane at $z = 0$. The black dashed curve a spherical cap fit to the interface contour. (C) Condensate-enriched tether concentration ψ_{l} increases with bulk tether concentration ψ_{g}, for different h_0, consistent with theory (solid curve, Eq. 3). (D) Contact angle $\cos\theta$ as a function of tether concentration ψ_{g} for different h_0, in agreement with theory (solid curves, Eq. 4). (E) $\cos\theta$ (Eq. 4) as functions of h_1 and ψ_{g}. $\cos = \pm 1$ represents wetting transitions to complete and no wetting, respectively. In all simulations, ψ follows Dirichlet boundary condition while ϕ follows no-flux boundary condition. See *SI Appendix* for details and parameters.

The presence of tethers reduces both surface tensions $\sigma_{\text{sl}} = \ln(1-\psi_{\text{l}}) - h_0\phi_{\text{l}}$ and $\sigma_{\text{sg}} = \ln(1-\psi_{\text{g}}) - h_0\phi_{\text{g}}$. However, the decrease in σ_{sl} is more substantial due to tether enrichment in the condensate ($\psi_{\text{l}} > \psi_{\text{g}}$). This, in turn, modifies the contact angle θ, which is determined by force balance at the three-phase junction: $\sigma_{\text{lg}} \cos\theta = \sigma_{\text{sg}} - \sigma_{\text{sl}}$. The modified contact angle is (see *SI Appendix* for details)

$$\cos\theta = \frac{\sigma_{\text{sg}} - \sigma_{\text{sl}}}{\sigma_{\text{lg}}} = \frac{\Delta\sigma_0 + \Delta\sigma_1}{\sigma_{\text{lg}}}, \tag{4}$$

where $\Delta\sigma_0 = h_0\Delta\phi$ is the surface tension difference in the absence of tethers, and $\Delta\sigma_1 = \ln\left[1+\psi_g(e^{h_1\Delta\phi}-1)\right]$ is the additional surface tension difference due to mobile tethers. $\Delta\sigma_1$ increases monotonically with tether abundance ψ_g and tether-condensate interaction h_1. Indeed, numerical simulations find the contact angle in simulations to be in excellent agreement with Eq. 4 (Fig. 1D, solid curves). Therefore, an attractive interaction due to mobile tethers can modulate wetting over a wide range of contact angles.

Wetting transitions occur at $\cos\theta = 1$, when a droplet completely wets the membrane, and at $\cos\theta = -1$, when a droplet detaches from the membrane (non-wetting). Tethers can induce transitions between these wetting regimes: For a repelling membrane that is initially in the non-wetting regime ($h_0 < -\sigma_{lg}/\Delta\phi$), both partial wetting [$\cos\theta \in (-1,1)$] and complete wetting ($\cos\theta = 1$) regimes can be achieved via a high enough density of attractive tethers (Fig. 1E). To reach complete wetting, the critical density of tethers required is $\psi_{g,c} = \frac{e^{\sigma_{lg}-h_0\Delta\phi}-1}{e^{h_1\Delta\phi}-1}$, which must stay below 1 since ψ is defined in terms of volume fractions. Since $\psi_{g,c}$ vanishes in the limit of large h_1, a finite number of tethers is sufficient to access all three wetting regimes as long as the tether-condensate attraction is strong enough.

For real tether molecules, how much binding energy is required to make a significant difference in wetting properties? Typically, the membrane would be slightly repulsive for polymer condensates because being close to the membrane reduces the conformational entropy of the polymers, leading to an estimated $\Delta\sigma_0 \sim -10^{-1}k_BT/\text{nm}^2$ [11]. In aqueous buffer, the condensate surface tension is of the same order $\sigma_{lg} \sim 10^{-1}k_BT/\text{nm}^2$ [12]. Thus, to drive wetting, tethers must reduce surface tension by the same order $\Delta\sigma_1 \sim 10^{-1}k_BT/\text{nm}^2$. A typical tether density of $n_g \sim 10^{-2}\text{nm}^2$ [13] yields a required binding energy of $\epsilon \approx \mathcal{O}(1)k_BT$ (see *SI Appendix* for details). Despite being a rough estimate, these calculations show that a reasonably modest per-tether binding energy (a few k_BT) could modulate wetting transitions.

Thus far, we have focused on the equilibrium morphologies due to tether-mediated wetting. But do tethers affect the dynamics of condensate formation and localization? In the alga *C. reinhardtii*, for example, the pyrenoid condensate dissolves and reforms every cell division, and the new pyrenoid centers around a reticulated region where many tubules meet. Hence, we hypothesize that mobile tethers may facilitate condensate localization by enrichment in the reticulated region. To illustrate this mechanism, we study a two-dimensional system which is bounded by membranes on the left and bottom sides and closed on the other two (Fig. 2). The bottom-left corner is favorable for the condensate since it can interact with the largest amount of membrane area

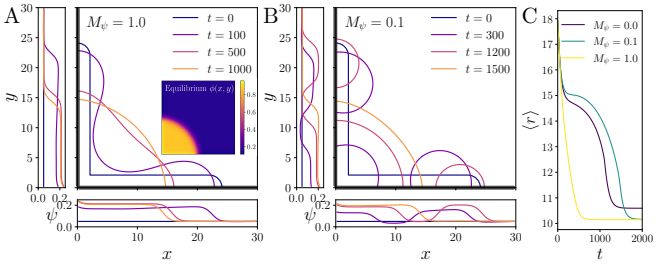

FIG. 2. (A–B) Dynamics of condensate localization for tether mobility $M_\psi = 1.0$ (A) and $M_\psi = 0.1$ (B). The simulation domain is a 2D system (x, y) with membranes on the left and bottom boundaries (indicated by thick black lines). Different colors indicate concentration profiles at different times (legend), with the condensate ϕ represented by interface contours and the tether ψ shown in the left and bottom insets. Inset in (A) shows the final equilibrium profile for $\phi(x, y)$. The tether density at the boundaries is $\psi_g = 0.05$. The overall $\langle\phi\rangle$ is conserved due to no-flux boundary conditions. (C) Condensate location as quantified by the average distance $\langle r\rangle = \int \delta\phi(x,y)\sqrt{x^2+y^2}\,dx\,dy \,/ \int \delta\phi(x,y)\,dx\,dy$, where $\delta\phi = \phi - \phi_g$. See *SI Appendix* for details.

(and therefore tethers), analogous to the reticulated region in the pyrenoid. Initially, the condensate coats part of the membrane, and its bulk concentration is between binodal and spinodal concentrations. If tethers have a high mobility, they quickly enrich in the condensate and help it localize to the corner (Fig. 2A). In contrast, if the tether mobility is low, the condensate first breaks up into smaller droplets, albeit eventually localizing to the corner through a coarsening process (Fig. 2B). Even though both reach the same equilibrium state, the latter process is much slower (Fig. 2C). Thus, by helping the condensate to optimize its membrane contacts, mobile tethers can facilitate coarsening and localization with respect to membrane structures, such as the tubules traversing the pyrenoid.

In summary, mobile tether molecules play an important role in mediating interactions between biomolecular condensates and membrane structures. Here, we developed a general theoretical framework to elucidate how mobile tethers affect both equilibrium and dynamical aspects of condensate wetting, which is relevant for a wide range of biological systems, including the algal pyrenoid [6, 7]. It will be important to further test the theory experimentally, for example, in systems such as supported lipid bilayers (e.g., fluorescently tagged tethers of known condensate affinities). More broadly, this framework can be extended to include effects such as membrane deformation and hydrodynamic coupling, as well as active processes, such as post-translational modification upon wetting. Overall, our framework paves the way for the study of how mobile-tether-mediated interactions affect condensate morphology and dynamics.

Acknowledgements—We thank B. Davidovitch, M. Jonikas, A. Martínez-Calvo, and N. Menon for useful discussions. This work was supported by a Harold W. Dodds Fellowship (Q.Y.), by NIH grant R01GM140032, by NSF grant MCB-2410354, by the Center for the Physics of Biological Function (NSF PHY-1734030), and by the Princeton Center for Complex Materials (NSF DMR-2011750).

[1] Y. Shin and C. P. Brangwynne, Liquid phase condensation in cell physiology and disease, Science **357**, eaaf4382 (2017).

[2] Q. Xiao, C. K. McAtee, and X. Su, Phase separation in immune signalling, Nature Reviews Immunology **22**, 188 (2022).

[3] Y. G. Zhao and H. Zhang, Phase separation in membrane biology: the interplay between membrane-bound organelles and membraneless condensates, Developmental Cell **55**, 30 (2020).

[4] A. Mangiarotti and R. Dimova, Biomolecular condensates in contact with membranes, Annual Review of Biophysics **53** (2024).

[5] V. Swaminathan, R. S. Fischer, and C. M. Waterman, The fak-arp2/3 interaction promotes leading edge advance and haptosensing by coupling nascent adhesions to lamellipodia actin, Mol. Biol. Cell **27**, 1085 (2016).

[6] J. H. Hennacy, N. Atkinson, A. Kayser-Browne, S. L. Ergun, E. Franklin, L. Wang, S. Eicke, Y. Kazachkova, M. Kafri, F. Fauser, J. Vilarrasa-Blasi, R. E. Jinkerson, S. C. Zeeman, A. J. McCormick, and M. C. Jonikas, Saga1 and mith1 produce matrix-traversing membranes in the co2-fixing pyrenoid, Nat. Plants **10**, 2038 (2024).

[7] M. T. Meyer, A. K. Itakura, W. Patena, L. Wang, S. He, T. Emrich-Mills, C. S. Lau, G. Yates, L. C. M. Mackinder, and M. C. Jonikas, Assembly of the algal co2-fixing organelle, the pyrenoid, is guided by a rubisco-binding motif, Sci. Adv. **6**, eabd2408 (2020).

[8] T. Young, Iii. an essay on the cohesion of fluids, Philosophical transactions of the royal society of London , 65 (1805).

[9] P. C. Hohenberg and B. I. Halperin, Theory of dynamic critical phenomena, Rev. Mod. Phys. **49**, 435 (1977).

[10] S. Mao, D. Kuldinow, M. P. Haataja, and A. Košmrlj, Phase behavior and morphology of multicomponent liquid mixtures, Soft Matter **15**, 1297 (2019).

[11] H. Hofmann, A. Soranno, A. Borgia, K. Gast, D. Nettels, and B. Schuler, Polymer scaling laws of unfolded and intrinsically disordered proteins quantified with single-molecule spectroscopy, Proc. Natl. Acad. Sci. U. S. A. **109**, 16155 (2012).

[12] H. Wang, F. M. Kelley, D. Milovanovic, B. S. Schuster, and Z. Shi, Surface tension and viscosity of protein condensates quantified by micropipette aspiration, Biophysical Reports **1** (2021).

[13] D. N. Itzhak, S. Tyanova, J. Cox, and G. H. Borner, Global, quantitative and dynamic mapping of protein subcellular localization, elife **5**, e16950 (2016).

Supplemental Material: Membrane wetting by biomolecular condensates is facilitated by mobile tethers

Trevor GrandPre,[1,2,*] Qiwei Yu,[1,*] Andrew G.T. Pyo,[2] Andrej Košmrlj,[3,4,†] and Ned S. Wingreen[1,5,‡]

[1] *Lewis-Sigler Institute for Integrative Genomics, Princeton University, Princeton, NJ 08544*
[2] *Department of Physics, Princeton University, Princeton, NJ 08544*
[3] *Department of Mechanical and Aerospace Engineering, Princeton University, Princeton, NJ 08544*
[4] *Princeton Materials Institute, Princeton University, Princeton, NJ 08544*
[5] *Department of Molecular Biology, Princeton University, Princeton, NJ 08544*

CONTENTS

I. THEORETICAL FRAMEWORK

As discussed in the main text, we consider a system where (three-dimensional) biomolecular condensates can interact with a (two-dimensional) membrane. The total free energy reads:

$$\beta F = c_{\psi,0}\int \mathrm{d}A\left[f_\psi(\psi)+\frac{\lambda_\psi}{2}(\nabla\psi)^2 - E(\psi,\phi|_{\mathrm{surf}})\right] + c_{\phi,0}\int \mathrm{d}V\left[f_\phi(\phi)+\frac{\lambda_\phi}{2}(\nabla\phi)^2\right], \tag{S1}$$

where ϕ is the condensate density field, ψ is the tether density field. The first integral is over the membrane area, while the second integral is over the bulk volume. $f_\phi(\phi)$ and $f_\psi(\psi)$ are the free energy densities of the condensate and tethers, respectively; $E(\psi,\phi|_{\mathrm{surf}})$ describes the interaction energy between the condensate and the tether/membrane, with $\phi|_{\mathrm{surf}}$ denoting the condensate density at the membrane surface. λ_ψ and λ_ϕ are related to the line/surface tensions. The free energy is measured in units of $\beta^{-1} = k_{\mathrm{B}}T$. The free energy densities (integrands in Eq. S1) are non-dimensionalized by the factor of β and reference concentrations $c_{\psi,0}$ and $c_{\phi,0}$, for the tether and the condensate, respectively [1]. For qualitative analysis and for the sake of simplicity, we set $c_{\psi,0}k_{\mathrm{B}}T = 1$ and $c_{\phi,0}k_{\mathrm{B}}T = 1$; this does not affect the qualitative results but must be revisited when estimating the energy scales for real tethers (Sec. II).

To minimize the free energy, we prescribe the following gradient (model-B) dynamics for both the tethers and condensate [2]:

$$\partial_t\psi = \nabla\cdot(M_\psi\nabla\mu_\psi), \quad \partial_t\phi = \nabla\cdot(M_\phi\nabla\mu_\phi), \tag{S2}$$

where M_ψ and M_ϕ are the mobility coefficients, and $\mu_\psi = \delta F/\delta\psi$ and $\mu_\phi = \delta F/\delta\phi$ are the chemical potentials of the tethers and condensate, respectively. The condensate obeys no-flux boundary condition at the membrane surface:

$$\partial_z\mu_\phi|_{z=0} = 0, \tag{S3}$$

where z is the normal vector pointing out of the membrane[1]. Additionally, the bulk-surface interaction gives the following wetting boundary condition:

$$\lambda_\phi\partial_z\phi|_{z=0} = -\partial_\phi E(\psi,\phi|_{z=0}), \tag{S4}$$

---

* These authors contributed equally to this work.
† andrej@princeton.edu
‡ wingreen@princeton.edu

[1] From now on, we will use $\cdots|_{z=0}$ and $\cdots|_{\mathrm{surf}}$ interchangeably to denote the values at the membrane surface.

which reflects a local change in condensate concentration near the membrane surface due to the condensate's interaction with the membrane and tethers.

While the model can be used to describe a large class of systems by allowing the free energy densities $f_\phi(\phi)$ and $f_\psi(\psi)$ and the interaction energy $E(\psi, \phi|_{\rm surf})$ to take different forms, we will focus on a minimal model to illustrate the essential physical picture.

A. A minimal model for tether-mediated wetting

For the sake of simplicity, we use Flory-Huggins free energy densities for both the condensate and the tethers

$$f_\psi(\psi) = \psi \ln \psi + (1-\psi)\ln(1-\psi) + \chi_\psi \psi(1-\psi), \tag{S5}$$
$$f_\phi(\phi) = \phi \ln \phi + (1-\phi)\ln(1-\phi) + \chi_\phi \phi(1-\phi), \tag{S6}$$

with ψ and ϕ denoting the area or volume fraction of tether and condensate, respectively. χ_ψ and χ_ϕ are the Flory-Huggins interaction parameters for the tether and the condensate, respectively.

We further assume a linear interaction energy (non-dimensionalized in the same way as f_ψ)

$$E(\psi, \phi) = (h_0 + h_1 \psi)\phi, \tag{S7}$$

where h_0 and h_1 describe condensate-membrane and condensate-tether interactions, respectively. The chemical potentials are given by:

$$\mu_\psi = \frac{\delta F}{\delta \psi} = \ln \frac{\psi}{1-\psi} + \chi_\psi(1-2\psi) - \lambda_\psi \nabla^2 \psi - h_1 \phi|_{z=0}, \tag{S8}$$
$$\mu_\phi = \frac{\delta F}{\delta \phi} = \ln \frac{\phi}{1-\phi} + \chi_\phi(1-2\phi) - \lambda_\phi \nabla^2 \phi. \tag{S9}$$

Further assuming that tethers do not interact with each other and only interact with the condensate, we have $\chi_\psi = 0$ and $\lambda_\psi = 0$. The tether chemical potential then simplifies to

$$\mu_\psi = \ln \frac{\psi}{1-\psi} - h_1 \phi|_{z=0}. \tag{S10}$$

Let $\phi_{\rm l}$ and $\phi_{\rm g}$ denote condensate densities in the dense (liquid) phase and the dilute (gas) phase, respectively. The corresponding tether densities in the dense and dilute phases are denoted as $\psi_{\rm l}$ and $\psi_{\rm g}$. They are related to each other through chemical potential balance:

$$\mu_{\psi,{\rm l}} = \mu_{\psi,{\rm g}} \Rightarrow \ln \frac{\psi_{\rm l}}{1-\psi_{\rm l}} - h_1 \phi_{\rm l}|_{z=0} = \ln \frac{\psi_{\rm g}}{1-\psi_{\rm g}} - h_1 \phi_{\rm g}|_{z=0}. \tag{S11}$$

Approximating the surface density $\phi|_{z=0}$ with the bulk binodal values[2], we have

$$\ln \frac{\psi_{\rm l}}{1-\psi_{\rm l}} = \ln \frac{\psi_{\rm g}}{1-\psi_{\rm g}} + h_1 \Delta\phi, \tag{S12}$$

where $\Delta\phi = \phi_{\rm l}|_{z=0} - \phi_{\rm g}|_{z=0} \approx \phi_{\rm l} - \phi_{\rm g}$ is the difference between binodal concentrations. Solving for $\psi_{\rm l}$:

$$\psi_{\rm l} = \frac{\psi_{\rm g} e^{h_1 \Delta\phi}}{1 + \psi_{\rm g}(e^{h_1 \Delta\phi} - 1)}, \tag{S13}$$

which produces Eq. (3) in the main text.

The contact angle θ is given by force balance at the three-phase junction:

$$\sigma_{\rm lg} \cos\theta = \sigma_{\rm sg} - \sigma_{\rm sl} \equiv \Delta\sigma, \tag{S14}$$

---

[2] The correction due to this approximation is $\mathcal{O}(h_0^2, h_1^2)$, which, as shown below, is a higher-order term.

where σ represents surface tensions. σ_{lg} is the surface tension between the dense and dilute phases in 3D and is independent of the tether concentration. The surface tension with the membrane σ_{s*}, which depends on the tether density ψ, is given by computing the excess free energy (per unit area):

$$\sigma_{s*} = f_\psi(\psi_*) + E(\psi_*, \phi_*|_{z=0}) - \mu_{\psi,*}\psi_* + \Delta f_{\mathrm{excess}}(\psi_*, \phi_*) \equiv \tilde{\sigma}_{s*} + \Delta f_{\mathrm{excess}}(\psi_*, \phi_*), \tag{S15}$$

where $* \in \{\mathrm{l}, \mathrm{g}\}$ denotes the dense ("liquid") or dilute ("gas") phase, respectively. $\mu_{\psi,*} = \ln \frac{\psi_*}{1-\psi_*} - h_1\phi_*|_{z=0}$ is the tether chemical potential. $\Delta f_{\mathrm{excess}}(\psi_*, \phi_*)$ is defined below and will prove to be higher order in h_0 and h_1. We define $\tilde{\sigma}_{s*}$ to be the sum of the first three terms, which is given by

$$\begin{aligned}
\tilde{\sigma}_{s*} =& f_\psi(\psi_*) + E(\psi_*, \phi_*|_{z=0}) - \mu_{\psi,*}\psi_* && \text{(S16)}\\
=& \psi_* \ln \psi_* + (1-\psi_*)\ln(1-\psi_*) - (h_0 + h_1\psi_*)\phi_* - \psi_*\left(\ln \frac{\psi_*}{1-\psi_*} - h_1\phi_*\right) && \text{(S17)}\\
=& \ln(1-\psi_*) - h_0\phi_*. && \text{(S18)}
\end{aligned}$$

The surface tension difference due to these terms reads

$$\Delta\tilde{\sigma} \equiv \tilde{\sigma}_{\mathrm{sg}} - \tilde{\sigma}_{\mathrm{sl}} = h_0(\phi_{\mathrm{l}} - \phi_{\mathrm{g}}) + \ln \frac{1-\psi_{\mathrm{g}}}{1-\psi_{\mathrm{l}}} = h_0(\phi_{\mathrm{l}} - \phi_{\mathrm{g}}) + \ln\left[1 + \psi_{\mathrm{g}}(e^{h_1\Delta\phi} - 1)\right] \equiv \Delta\sigma_0 + \Delta\sigma_1, \tag{S19}$$

where $\Delta\sigma_0 = h_0(\phi_{\mathrm{l}} - \phi_{\mathrm{g}}) = h_0\Delta\phi$ is the surface tension difference in the absence of tethers, and $\Delta\sigma_1 = \ln\left[1 + \psi_{\mathrm{g}}(e^{h_1\Delta\phi} - 1)\right]$ is the additional surface tension difference due to mobile tethers. We have substituted ψ_{l} with Eq. S13. Note that to the leading order, we have $\Delta\tilde{\sigma} = \mathcal{O}(h_0, h_1)$.

$\Delta f_{\mathrm{excess}}(\psi_*, \phi_*|_{z=0})$ is the excess free energy density due to a boundary layer of condensates at the membrane surface, where the condensate concentration profile $\phi(z)$ deviates from the binodal:

$$\Delta f_{\mathrm{excess}}(\psi_*, \phi_*) = \int \mathrm{d}z_1 \left[g_\phi(\phi_*(z_1)) + \frac{\lambda_\phi}{2}(\partial_z\phi_*(z_1))^2 - g_\phi(\phi_*)\right], \tag{S20}$$

where ϕ_* denotes the binodal concentration, and $g_\phi(\phi) = f_\phi(\phi) - \mu_\phi\phi$ is the Gibbs free energy of the condensate. The concentration profile $\phi_*(z_1)$ is the solution to the following boundary value problem:

$$\begin{aligned}
\partial_z\mu_\phi(z_1) &= 0, \quad z_1 > 0, && \text{(S21)}\\
\lambda_\phi\partial_z\phi_*(z_1) &= -(h_0 + h_1\psi_*), \quad z_1 = 0, && \text{(S22)}\\
\lim_{z_1\to\infty} \phi_*(z_1) &= \phi_*. && \text{(S23)}
\end{aligned}$$

In practice, we find that the excess free energy density is negligible compared to the other terms. This can be explained by the following scaling argument: To the leading order in $\delta\phi_*(z) = \phi_*(z) - \phi_*$, the excess free energy is

$$\Delta f_{\mathrm{excess}} \sim \frac{\Delta z}{2} \cdot \left[\lambda_\phi\delta\phi_*'(z)^2 + g''(\phi)\delta\phi_*(z)^2\right] = \mathcal{O}(\delta\phi_*^2), \tag{S24}$$

where Δz is the boundary layer thickness, and we have used $g'(\phi) = 0$ at the binodal concentration. From the wetting condition [Eq. S22], we find $\delta\phi_* = \mathcal{O}(h_0, h_1)$. Hence, the excess free energy becomes quadratic in the interaction parameters:

$$\Delta f_{\mathrm{excess}} = \mathcal{O}\big(h_0^2, h_1^2\big), \tag{S25}$$

which is a higher-order term compared to $\Delta\tilde{\sigma}$.

Putting everything together:

$$\cos\theta = \frac{\sigma_{\mathrm{sg}} - \sigma_{\mathrm{sl}}}{\sigma_{\mathrm{lg}}} \approx \frac{\Delta\tilde{\sigma}}{\sigma_{\mathrm{lg}}} = \frac{\Delta\sigma_0 + \Delta\sigma_1}{\sigma_{\mathrm{lg}}} = \frac{h_0(\phi_{\mathrm{l}} - \phi_{\mathrm{g}}) + \ln\left[1 + \psi_{\mathrm{g}}(e^{h_1\Delta\phi} - 1)\right]}{\sigma_{\mathrm{lg}}}, \tag{S26}$$

which produces Eq. (4) in the main text.

To achieve complete wetting ($\cos\theta = 1$), the critical tether density $\psi_{\mathrm{g,c}}$ is given by

$$\sigma_{\mathrm{lg}} = h_0\Delta\phi + \ln\left[1 + \psi_{\mathrm{g,c}}(e^{h_1\Delta\phi} - 1)\right] \Rightarrow \psi_{\mathrm{g,c}} = \frac{e^{\sigma_{\mathrm{lg}} - h_0\Delta\phi} - 1}{e^{h_1\Delta\phi} - 1}. \tag{S27}$$

II. ESTIMATING THE TETHER BINDING ENERGY REQUIRED TO DRIVE WETTING TRANSITION

Here, we estimate the value of $\Delta\sigma_0$, which is the dilute/dense phase surface tension difference due to the condensate-membrane interaction. Typically, the membrane would be slightly repulsive for polymer condensates because being close to the membrane reduces the conformational entropy of the polymers. Thus, we can estimate the magnitude of this effect by considering polymer "blobs" close to the membrane. Each "blob" would contribute $1k_BT$, and the number of polymer "blobs" per unit area could be estimated by $1/R_g^2$ with R_g being the radius of gyration. For an IDP of length ~ 100 a.a., we estimate $R_g \sim 3$nm [3], and therefore $1/R_g^2 \sim \mathcal{O}(10^{-1})\text{nm}^2$. Thus, the surface tension due to entropic repulsion is of the order $\Delta\sigma_0 \sim -\mathcal{O}(10^{-1})k_BT/\text{nm}^2$.

On the other hand, previous micropipette aspiration found that the condensate surface tension σ_{lg} is at most $\mathcal{O}(1)$mN/m, or equivalently $\mathcal{O}(10^{-1})k_BT/\text{nm}^2$. Thus, to achieve complete wetting, the additional surface tension difference due to tethers must also reach $\Delta\sigma_1 = \sigma_{lg} - \Delta\sigma_0 \sim \mathcal{O}(10^{-1})k_BT/\text{nm}^2$.

To estimate the binding energy relevant for real tethers, we recall that the surface tension was renormalized by $c_{\psi,0}k_BT$, with a close-packed tether density set by $c_{\psi,0}$. Thus, in the limit of dilute tethers $\psi_g = n_g/c_{\psi,0} \ll 1$, where n_g is the (dimensional) tether density in contact with the dilute phase, we have

$$\frac{\Delta\sigma_1}{k_BT} = c_{\psi,0}\ln\left[1+\psi_g(e^{h_1\Delta\phi}-1)\right] \approx c_{\psi,0}\psi_g(e^{h_1\Delta\phi}-1) = n_g(e^{\epsilon}-1), \tag{S28}$$

where $n_g \sim 10^{-2}\text{nm}^2$ [4] is the tether number density, and $\epsilon = h_1\Delta\phi$ is the energy reduction per tether when inside the condensate, measured in units of k_BT. This lead to

$$\epsilon = \ln\left(1+\frac{\Delta\sigma_1}{n_g k_BT}\right) \sim \ln\left[1+\mathcal{O}(10)\right] \sim \mathcal{O}(1)\ (k_BT), \tag{S29}$$

which suggests that a binding energy of a few k_BT per tether is relevant for modulating the equilibrium wetting properties.

III. DETAILS OF NUMERICAL SIMULATIONS

To solve the equations of motion (Eq. S2) for the condensate and tethers, we use a finite-flux numerical scheme with first-order forward Euler time-stepping for time evolution. The condensate field ϕ obeys no-flux boundary conditions at all boundaries in addition to wetting boundary conditions at membrane interfaces. The tether field ψ obeys Dirichlet boundary conditions with fixed bulk tether concentration ψ_g.

For Fig. 1, the simulation was performed in cylindrical coordinates, with spatial discretization $r_n = \frac{nr_{\max}}{N}$, $z_m = \frac{mz_{\max}}{M}$, where $r_{\max} = 60$ and $z_{\max} = 40$ set the system size and $N = M = 128$ set the spatial resolution. The system was evolved to its equilibrium state. The contact angle is measured by fitting the contour to a spherical cap $R^2 = r^2 + (z-z_0)^2$, which gives $\cos\theta = -z_0/R_0$. The parameters are: $\chi_\phi = 2.5$, $\lambda_\phi = 1$, $\chi_\psi = 0$, $\lambda_\psi = 0$; $h_1 = 1$ for (B)–(D); $\psi_g = 0.02$ and $h_0 = 0$ for (B); $h_0 = -0.2$ for (E).

For Fig. 2, the simulation was performed in 2D planar coordinates, with spatial discretization $x_n = \frac{nx_{\max}}{N}$, $y_m = \frac{my_{\max}}{M}$ with $x_{\max} = y_{\max} = 30$ and $N = M = 64$. The parameters are: $h_0 = -0.2$, $h_1 = 2$, $\chi_\phi = 2.5$, $\lambda_\phi = 1$, $\chi_\psi = 0$, $\lambda_\psi = 0$. Tether concentration is fixed at the boundary by Dirichlet boundary condition $\psi_g = 0.05$.

To quantify how fast the droplet reaches its equilibrium configuration at the lower-left corner where the two membranes meet, we defined an average distance $\langle r\rangle = \int \delta\phi(x,y)\sqrt{x^2+y^2}\,\mathrm{d}x\,\mathrm{d}y \,/\, \int \delta\phi(x,y)\,\mathrm{d}x\,\mathrm{d}y$, where $\delta\phi = \phi - \phi_g$ is the condensate concentration subtracted by the dilute phase.

REFERENCES

[1] S. Mao, D. Kuldinow, M. P. Haataja, and A. Košmrlj, Phase behavior and morphology of multicomponent liquid mixtures, Soft Matter **15**, 1297 (2019).
[2] P. C. Hohenberg and B. I. Halperin, Theory of dynamic critical phenomena, Rev. Mod. Phys. **49**, 435 (1977).
[3] H. Hofmann, A. Soranno, A. Borgia, K. Gast, D. Nettels, and B. Schuler, Polymer scaling laws of unfolded and intrinsically disordered proteins quantified with single-molecule spectroscopy, Proc. Natl. Acad. Sci. U. S. A. **109**, 16155 (2012).
[4] D. N. Itzhak, S. Tyanova, J. Cox, and G. H. Borner, Global, quantitative and dynamic mapping of protein subcellular localization, elife **5**, e16950 (2016).